Planar waveguide-coupled, high-index-contrast, high-Q resonators in chalcogenide glass for sensing

Planar waveguide-coupled, high-index-contrast, high-Q resonators in chalcogenide glass for sensing

Juejun Hu,[1,*] Nathan Carlie,[2] Ning-Ning Feng,[1] Laeticia Petit,[2] Anu Agarwal,[1] Kathleen Richardson,[2] and Lionel Kimerling[1]

[1]*Microphotonics Center, Massachusetts Institute of Technology, Cambridge, MA 02139, USA*

[2]*School of Materials Science and Engineering, COMSET, Clemson University, Clemson, SC 29634, USA*

[*]*Corresponding author: hujuejun@mit.edu*

High-index-contrast, compact microdisk resonators in thermally evaporated As_2S_3 and $Ge_{17}Sb_{12}S_{71}$ chalcogenide glass films are designed, fabricated using standard UV lithography and characterized. Our pulley coupler configuration demonstrates coupling of the resonators to monolithically integrated photonic wire waveguides without resorting to demanding fine-line lithography. Microdisk resonators in As_2S_3 support whispering-gallery-mode with cavity quality factors (Q) exceeding 2×10^5, the highest Q value reported in resonator structures in chalcogenide glasses to the best of our knowledge. We have successfully demonstrated a *lab-on-a-chip* prototype sensor device with the integration of our resonator with planar microfluidic systems. The sensor shows a refractive index sensitivity of 182 nm/RIU (refractive index unit) and a wavelength resolution of 0.1 pm through resonant peak fit. This corresponds to a refractive index detection limit of 8×10^{-7} RIU at 1550 nm wavelength, which could be further improved

by shifting the operating wavelength to a region where water absorption is reduced.

OCIS codes: 130.3120, 130.2755, 130.6010, 160.2750, 130.4310, 280.1415, 120.5710.

Integrated resonator structures are attracting considerable interest lately due to their unique capability of confining photons in a small volume for an extended period of time, thereby leading to strong resonant enhancement of field intensity. Chalcogenide glasses have high Kerr nonlinearity and wide infrared transparency, making them superior for nonlinear optics and sensing [1]. In addition, their high refractive index allows small cavity mode volume without suffering from excess radiative loss. However, in such high-index-contrast (HIC) systems, the gap between the resonator and its bus waveguide typically has to be smaller than a few hundred nanometers to guarantee sufficient coupling [2]. This requirement poses a significant fabrication challenge. High-cost fine-line patterning techniques such as electron beam lithography or focus-ion-beam milling are labor intensive but often become necessary for device fabrication. A racetrack ring design partially resolves the fabrication issue due to the increased coupling length; however, it also increases cavity mode volume and induces additional loss due to abrupt changes of waveguide bending curvature.

In this letter, we present the fabrication and characterization of integrated HIC microdisk resonators in thermally evaporated As_2S_3 and $Ge_{17}Sb_{12}S_{71}$ glasses. A pulley coupler design improves coupling efficiency and relieves the stringent fabrication tolerances, potentially allowing the fabrication of HIC glass resonators using simple, low-cost standard UV aligner lithography. Whispering-gallery-mode (WGM) in As_2S_3 microdisk resonators exhibits cavity Q

factors as high as 210,000. The Q value represents a 20-fold improvement compared to our recently demonstrated racetrack rings [3], and is 2.5 times that of chalcogenide glass microspheres [4].

Such structures enable application in a diverse range of systems. High-Q optical resonators have been recognized as a promising device platform for biochemical sensing, taking advantage of the strong photon-matter interaction induced by optical resonance in micro-cavities [5-8]. Additionally, microfluidics and its integration onto a chip with other components will give rise to advances in an emerging field that may revolutionize chemical and biological analysis. Integration of different liquid-handling functionalities onto a single chip (thus named "lab-on-a-chip") will result in devices and systems capable of detecting a range of target species for a diverse cross-section of applications. Further, high liquid flow velocity in a microfluidic channel leads to hydrodynamic thinning of boundary layers on sensor surface, which facilitates molecular diffusion and reduces sensor response time [9]. We demonstrate integration of $Ge_{17}Sb_{12}S_{71}$ microdisk resonators with PDMS (polydimethylsiloxane) microfluidic channels, and show that the microfluidic device can be used as highly sensitive refractive index sensors.

The bulk preparation and film deposition process used for resonator fabrication are described elsewhere [10-12]. The films are patterned by lift-off, with the complete patterning process realized on a 500 nm CMOS line [13]. The bus waveguides are comprised of photonic wires with a width of 800 nm, and microdisks and bus waveguides have a height of 450 nm for both compositions. To prevent surface oxidation of devices in As_2S_3, a 3 μm thick layer of SU8 polymer is spin-coated to serve as a top cladding after patterning and the As_2S_3 devices are subsequently annealed at 140˚C for 3 h to stabilize the glass structure, whereas no SU8 coatings are applied on $Ge_{17}Sb_{12}S_{71}$ resonators. Figure 1(a) shows the top view of a fabricated As_2S_3

microdisk resonator with a bus waveguide in a "pulley-type" coupling configuration. Compared to a conventional microdisk/micro-ring coupler, the pulley coupler design increases the coupling length leading to stronger coupling. As an example, Fig. 1(b) shows the simulated TE polarization external Q-factor (i.e. Q-factor due to coupling) and the corresponding coupled Q-factor at critical coupling (twice the external Q due to coupling alone) when the gap width is varied. The optical bending modes of the disk and the waveguide are calculated using a full-vectorial bending mode solver [14]. The computed fields are then substituted into the coupled-mode equation to calculate the coupling coefficients [15], and Q-factors are extracted based on the coupling coefficients using Little's formulation [16]. Figure 1(b) clearly shows that in order to achieve the same coupling strength as a conventional coupler design, a wider gap between a resonator and a bus waveguide is possible when a pulley coupler is employed. The smaller slope of the curve corresponding to the pulley coupler also suggests improved fabrication tolerance to gap width variations. With such performance constraints reduced, lower cost lithography techniques can be used to fabricate the structures.

The transmission spectra of the fabricated devices are measured on a Newport AutoAlign workstation in combination with a LUNA tunable laser (optical vector analyzer, LUNA Technologies, Inc.). Lens-tip fibers are used to couple light from the laser into and out of the devices. Reproducible coupling is achieved via an automatic alignment system with a spatial resolution of 50 nm. The sample is mounted on a thermostat stage and kept at 25 ˚C for all measurements. As_2S_3 and $Ge_{17}Sb_{12}S_{71}$ microdisks with a radius of 20 μm and varied waveguide-resonator gap separation from 500 nm to 1200 nm have been tested. Table 1 summarizes the optical properties of the resonators, and measured transmission spectra of an As_2S_3 microdisk with a gap separation of ~ 800 nm between bus waveguide and microdisk is shown in Fig. 3 as

an example. The transmission spectra feature a set of resonant peaks evenly spaced by a well-defined free spectral range, indicative of single-mode resonator operation. The microdisk operates near critical coupling regime for both TE and TM polarizations around 1550 nm wavelength, an important advantage for applications in the telecommunication bands. The higher Q factor of TM polarization suggests that bending loss is insignificant in the microdisk, and thus it is possible to achieve an even smaller cavity mode volume without suffering excess radiative loss. It should be noted however that a complete analysis of factors limiting the propagation loss and hence cavity Q-factor in these resonators is still under investigation.

$Ge_{17}Sb_{12}S_{71}$ microdisks are used for microfluidic integration given its superior chemical stability in air and in different chemical environments of interest for our sensing applications. PDMS (Sylgard 184 Silicone Elastomer, Dow Corning Inc.) microfluidic channels with a width of 100 μm and a height of 30 μm are fabricated via replica molding. After oxygen plasma treatment, the channels are irreversibly bonded onto the chips on which the microdisks are patterned. Liquid inlet and outlet access holes are punched prior to bonding, and PTFE (polytetrafluoroethene) tubing is attached into the access holes to complete the microfluidic chip fabrication. During testing, deionized (DI) water solutions of isopropanol (IPA) of varying concentrations are injected into the channels through a syringe pump, and the resonant peak shift due to ambient refractive index change is monitored *in situ*. The measurements with different concentrations of solutions are repeated twice to confirm reproducibility. TM polarization transmission spectra of a $Ge_{17}Sb_{12}S_{71}$ resonator in IPA solutions of various concentrations are shown in Fig. 3(a). The resonant wavelength shift as a function of IPA concentration and corresponding solution refractive index is plotted in Fig. 3(b), and a refractive index (RI)

sensitivity of (182 ± 5) nm/RIU is inferred from the fitted curve slope. The RI sensitivity can be also predicted using the equation below:

$$Sensitivity_{RI} = \frac{\lambda}{n_g} \times \Gamma_{iv} \quad (1)$$

where λ is the operating wavelength, Γ_{iv} denoted the TM mode power confinement factor in the interrogation volume (water solution in this case) estimated to be 0.204 using finite difference simulations and n_{eff} the modal effective index simulated to be 1.63. Based on the simulation results, an RI sensitivity of 194 nm/RIU is predicted. The difference between experimentally measured RI sensitivity and theoretical prediction is probably due to a slight deviation in waveguide dimension from the target design values.

By applying a Lorentzian fit to the resonant peaks, we show that the resonant wavelength can be determined to an accuracy of ~ 0.1 pm limited by noise [17]. Besides resonant wavelength shift, we observed that the cavity Q-factor decreased from 110,000 to 20,000 after solution injection, which can be directly attributed to the optical absorption of water. Using the absorption coefficient of water at 1550 nm wavelength (α = 9.6 cm^{-1} [18]), we estimate the absorption-limited Q-factor to be ~ 19,000, in excellent agreement with our measurement result. By shifting the operating wavelength to near infrared water transparency windows (e.g. 1.06 μm wavelength), we can expect minimized Q deterioration due to water absorption, which should lead to much higher sensor sensitivity [17].

In summary, we fabricate and characterize high-index-contrast, planar waveguide-coupled microdisk resonators in chalcogenide glasses with record cavity Q-factors. A pulley coupler design is employed to allow improved control on optical coupling into the resonator. We demonstrate photonic-microfluidic integration on the microdisk platform, and a prototypical

microfluidic refractive index sensor with an index detection limit of 8×10^{-7} RIU is presented. The microdisk device is a promising device platform for biochemical sensing and microphotonics integration.

Acknowledgment

Funding support is provided by the Department Of Energy under award number DE-SC52-06NA27341. The authors also acknowledge the Microsystems Technology Laboratories at MIT for fabrication facilities.

References

1. A. Greer and N. Mathur, "Materials science: Changing face of the chameleon," Nature **437**, 1246 (2005).

2. V. Almeida, C. Barrios, R. Panepucci, and M. Lipson, "All-optical control of light on a silicon chip," Nature **431**, 1081 (2004).
3. J. Hu, N. Carlie, L. Petit, A. Agarwal, K. Richardson, and L. Kimerling, "Demonstration of chalcogenide glass racetrack microresonators," Opt. Lett. **33**, 761 (2008).
4. G. Elliott, D. Hewak, G. Murugan, and J. Wilkinson, "Chalcogenide glass microspheres; their production, characterization and potential," Opt. Express **15**, 17542 (2007).
5. F. Vollmer, D. Braun, A. Libchaber, M. Khoshsima, I. Teraoka, and S. Arnold, "Protein detection by optical shift of a resonant microcavity," Appl. Phys. Lett. **80,** 4057 (2002).
6. A. Armani, R. Kulkarni, S. Fraser, R. Flagan, K. Vahala, "Label-Free, Single-Molecule Detection with Optical Microcavities," Science **317,** 7837 (2007).
7. C. Chao and L. Guo, "Biochemical sensors based on polymer microrings with sharp asymmetrical resonance," Appl. Phys. Lett. **83,** 1527 (2003).
8. Y. Sun, S. Shopova, G. Frye-Mason, and X. Fan, "Rapid chemical-vapor sensing using optofluidic ring resonators," Opt. Lett. **33,** 788 (2008).
9. R. Glaser, "Antigen-Antibody Binding and Mass Transport by Convection and Diffusion to a Surface: A Two-Dimensional Computer Model of Binding and Dissociation Kinetics," Anal. Biochem. **213**, 152 (1993).
10. L. Petit, N. Carlie, F. Adamietz, M. Couzi, V. Rodriguez, and K. C. Richardson, "Correlation between physical, optical and structural properties of sulfide glasses in the system Ge-Sb-S," Mater. Chem. Phys. **97**, 64 (2006).
11. W. Li, S. Seal, C. Rivero, C. Lopez, K. Richardson, A. Pope, A. Schulte, S. Myneni, H. Jain, K. Antoine, and A. Miller, "Role of S/Se ratio in chemical bonding of As-S-Se glasses

investigated by Raman, x-ray photoelectron, and extended x-ray absorption fine structure spectroscopies," J. Appl. Phys. **98**, 053503 (2005).

12. J. Hu, V. Tarasov, N. Carlie, L. Petit, A. Agarwal, K. Richardson, and L. Kimerling, "Fabrication and Testing of Planar Chalcogenide Waveguide Integrated Microfluidic Sensor," Opt. Express **15**, 2307 (2007).
13. J. Hu, V. Tarasov, N. Carlie, N. Feng, L. Petit, A. Agarwal, K. Richardson, and L. Kimerling, "Si-CMOS-compatible lift-off fabrication of low-loss planar chalcogenide waveguides," Opt. Express **15**, 11798 (2007).
14. N. Feng, G. Zhou, C. Xu, and W. Huang, "Computation of full-vector modes for bending waveguide using cylindrical perfectly matched layers," IEEE J. Lightwave Technol. **20**, 1976 (2002).
15. H. Haus, W. Huang, S. Kawakami, and N. Whitaker, "Coupled-mode theory of optical waveguides," IEEE J. Lightwave Technol. **5**, 16 (1987).
16. B. Little, S. Chu, H. Haus, J. Foresi, and J. Laine, "Microring resonator channel dropping filters," IEEE J. Lightwave Technol. **15**, 998 (1997).
17. J. Hu, X. Sun, A. Agarwal, and L. Kimerling, "Detection limit of optical resonator biochemical sensors," submitted to J. Opt. Soc. Am. B.
18. W. Irvine and J. Pollack, "Infrared optical properties of water and ice spheres," Icarus **8**, 324 (1968).

Table 1. Coupled cavity Q and free spectral range (FSR) of As_2S_3 and $Ge_{17}Sb_{12}S_{71}$ microdisk resonators with a 20 μm radius measured at critical coupling (quoted for resonant peaks with extinction ratios > 15 dB) near 1550 nm wavelength.

Composition	Cavity Q (± 10%)		FSR (nm)	
	TM	TE	TM	TE
As_2S_3	210,000	150,000	7.6	7.8
$Ge_{17}Sb_{12}S_{71}$ (in air)	110,000	100,000	8.3	8.9
$Ge_{17}Sb_{12}S_{71}$ (in water)	20,000		8.4	

Fig. 1. (color online) (a) Optical micrograph of a 20-μm-radius pulley-type As_2S_3 microdisk resonator: the gap separating the bus waveguide and the disk is ~ 800 nm wide; (b) Simulated TE mode external Q-factor and corresponding coupled Q-factor at critical coupling at a wavelength of 1550 nm as a function of gap width between the microdisk and a bus waveguide. In this simulation, the $Ge_{17}Sb_{12}S_{71}$ (refractive index 2.06) microdisk sits on an oxide (refractive index 1.45) under cladding and is immersed in water (refractive index 1.33). The disk has a radius of 20 μm, and both the bus waveguide and the disk have a height of 450 nm.

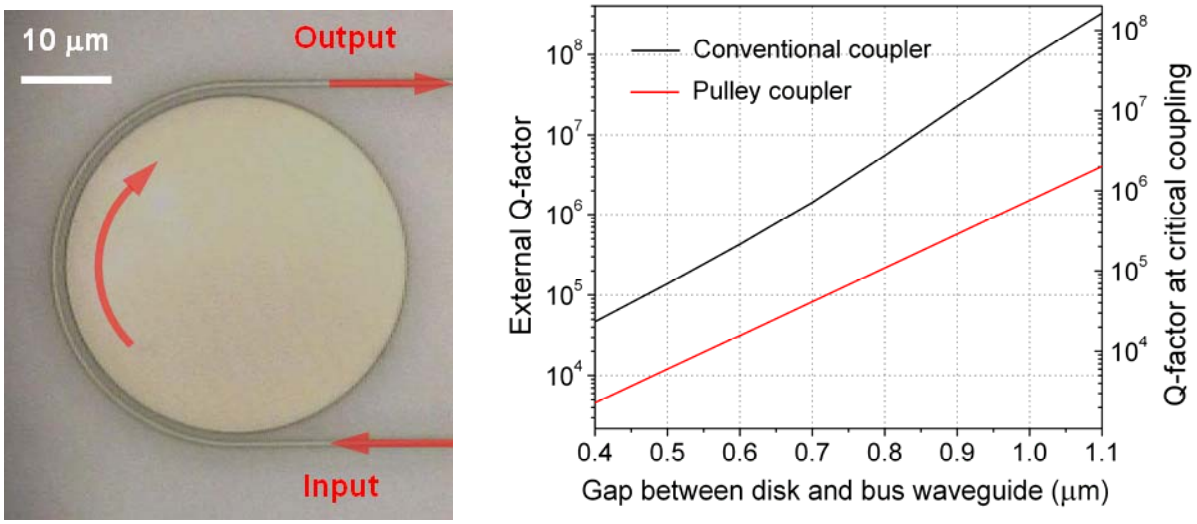

(a) (b)

Fig. 2. (color online) (a) Measured transmission spectra of a 20-μm-radius microdisk resonator; (b) A TM-polarization transmission spectrum averaged over 32 wavelength-sweeping scans near a resonant peak: the black dots are experimental data points and the red curve is the Lorentzian peak fitted in linear scale.

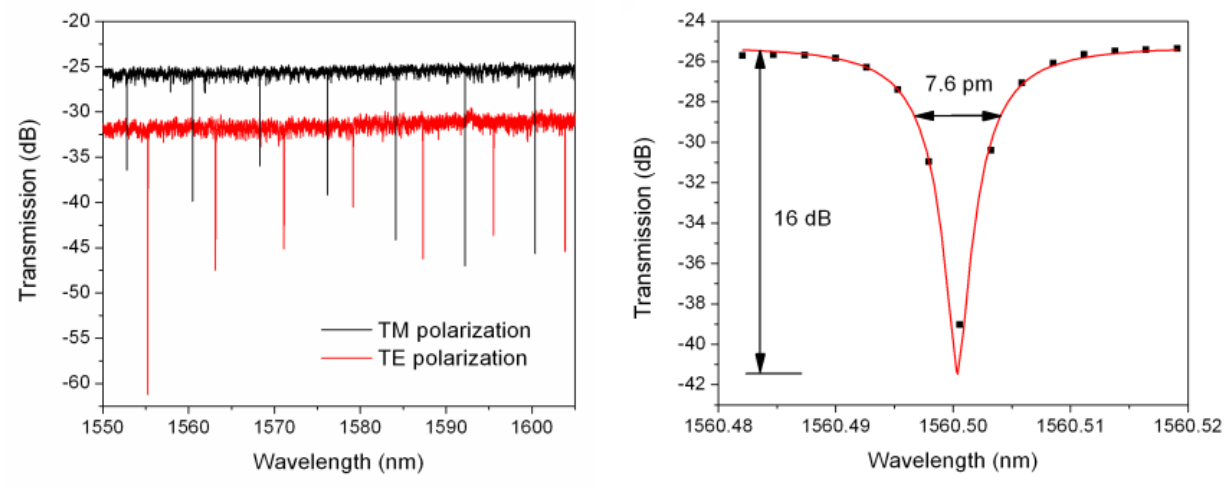

(a) (b)

Fig. 3. (color online) (a) TM polarization transmission spectra of a $Ge_{17}Sb_{12}S_{71}$ microdisk in IPA solutions with four different concentrations; (b) Measured resonant peak wavelength shift as a function of IPA solution mole ratio concentration and corresponding solution refractive index.

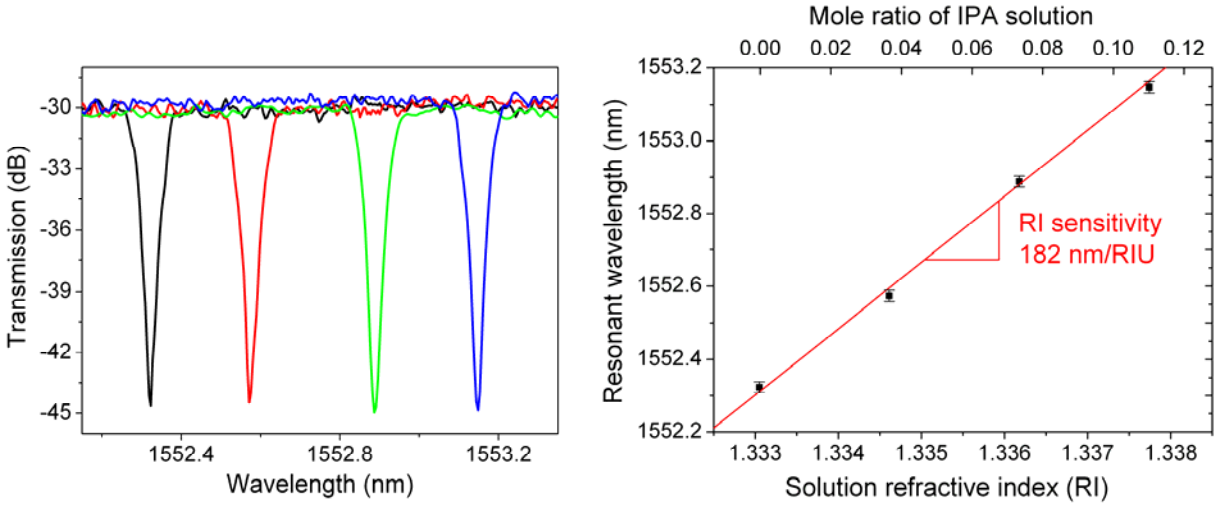

(a) (b)